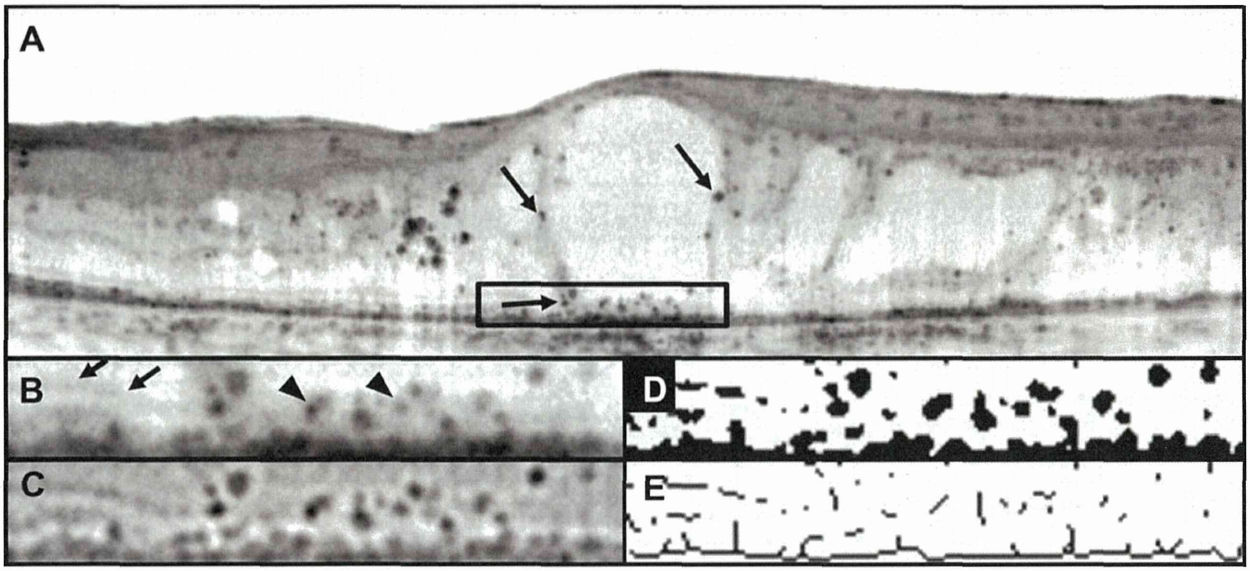

FIGURE 2. Calculation of parallelism through skeletonizing OCT images of the photoreceptor-RPE complex of a DME patient with hyperreflective foci in the outer retinal layers. Images are of the left eye of a 65-year-old man with DME. The Snellen equivalent BCVA was 20/50 in this eye. (**A**) A horizontal line scan of the SD-OCT image through the fovea shows cystoid macular edema and hyperreflective foci (*arrows*) in both the inner and outer retinal layers. The foveal thickness was 642 μm. (**B**) A magnified view of the area *outlined in black* in (**A**). The ELM line and inner segment ellipsoid line were disrupted and categorized as ELM line(±) and inner segment ellipsoid line(±), respectively. The ELM line sank and deformed toward the RPE (*arrow*). Hyperreflective foci (*arrowheads*) are observed in the area where the ELM line and inner segment ellipsoid line are absent, and some were deposited on the RPE. (**C**) A filtered image of (**B**) after the application of a band-pass filter for noise reduction and enhancement of the line segments. (**D**) A binarized image of (**C**) after using Otsu's thresholding method for automatic binarization level decisions. (**E**) A skeletonized image generated from (**D**). Line segments were observed in random orientations, which contributed to decreased parallelism. The parallelism value calculated for this area was 0.492.

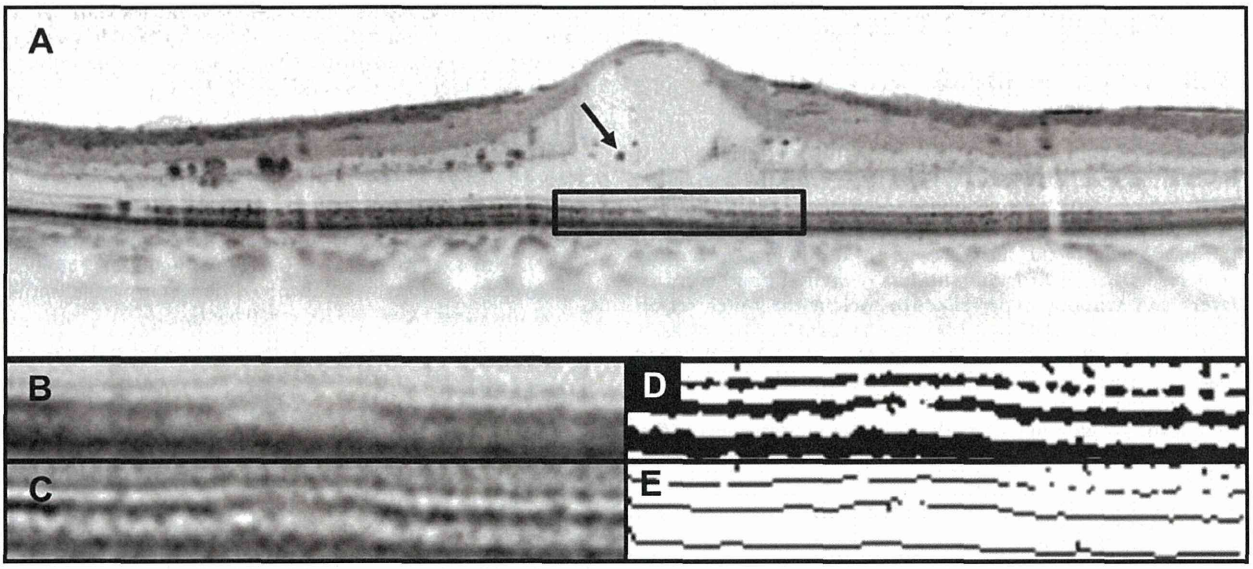

FIGURE 3. Calculation of parallelism through skeletonizing OCT images of the photoreceptor-RPE complex of a DME patient without hyperreflective foci in the outer retinal layers. Images are of the left eye of a 74-year-old man with DME. The Snellen equivalent BCVA was 20/25 in this eye. (**A**) A horizontal line scan of the SD-OCT image through the fovea shows cystoid macular edema and hyperreflective foci (*arrows*) in the inner retinal layers, but not in the outer retinal layers. The foveal thickness was 440 μm. (**B**) A magnified view of the area *outlined in black* in (**A**). The inner segment ellipsoid line was disrupted and categorized as ELM line(+) and inner segment ellipsoid line(±). Neither ELM line deformation nor hyperreflective foci are observed in the image. (**C**) The filtered image from (**B**) after the application of a band-pass filter for noise reduction and enhancement of the line segments. (**D**) A binarized image of (**C**) after using Otsu's thresholding method for automatic binarization level decisions. (**E**) A skeletonized image generated from (**D**). Line segments are depicted as almost parallel lines, and the parallelism calculated for this area was 0.689.

Investigative Ophthalmology & Visual Science

Table 1. Differences in Parallelism Between Healthy Subjects and Patients With DME in OCT Images

Characteristic	Normal Eyes	Eyes With DME	*P* Value
No. eyes/patients	30/30	90/79	—
Men/women	16/14	49/41	—
Age, y	63.0 ± 9.9	65.3 ± 8.6	0.2140
VA, logMAR	−0.153 ± 0.002	0.360 ± 0.104	<0.0001
Parallelism	0.745 ± 0.082	0.572 ± 0.151	<0.0001
Retinal thickness	259 ± 17	474 ± 117	<0.0001

parallelism than eyes with either an interrupted or absent inner segment ellipsoid line or ELM line. These results suggest that parallelism reflects assessments of inner segment ellipsoid line or ELM line continuity by graders. Meanwhile, the results also imply that inner segment ellipsoid line and ELM line continuity may be closely related to other components that decrease the image complexity of the photoreceptor-RPE complex, given that parallel discontinuous lines in the image cannot contribute to a decrease in parallelism per se. Parallelism has the potential to reflect structural changes in the photoreceptor-RPE complex, which include discontinuity of inner segment ellipsoid line or ELM line, among other changes.

One of the possible candidates that can decrease parallelism and show a relationship with photoreceptor layer discontinuity is the presence of hyperreflective foci in the outer retinal layers. As we previously reported, hyperreflective foci in the outer retinal layers, subclinical findings that are invisible during clinical ophthalmoscopic examinations, have been reported to have a pathological association with disrupted inner segment ellipsoid lines or ELM lines in SD-OCT images of eyes with DME.[22] In fact, in the current study, we identified a significant difference in parallelism between the groups with and without hyperreflective foci in the outer retinal layers. In eyes with hyperreflective foci in the outer retinal layers, the hyperreflective foci themselves and their deposits on the RPE line can contribute to irregular and bumpy RPE lines, and are considered to be skeletonized through image processing as random lines at angles to the inner segment ellipsoid lines or ELM lines.

Deformation of the ELM line, which can be often seen in DME, is another candidate that can decrease parallelism in eyes with DME. In cases with disrupted ELM lines, the ELM lines sometimes sank and merged with the RPE, as previously reported.[22] Because the ELM corresponds to the adherens junctions between the Müller cells and photoreceptor cells and acts as a barrier against macromolecules,[15] these deformations may represent cellular damage and can occur in association with ELM line discontinuity. Meanwhile, parallelism in cases with disrupted ELM or inner segment ellipsoid lines without any line deformation or hyperreflective foci may not be low values, as shown in Figure 3. However, considering the good association between grader-based evaluations of photoreceptor layer continuity and parallelism, increases in image complexity resulting from the above-mentioned presence of hyperreflective foci or ELM line deformation other than inner segment ellipsoid line or ELM line discontinuity may have the potential to be a comprehensive and useful sign that reflects damage to the outer retinal layers, at least in eyes with DME.

A number of studies have reported quantitative or automatic evaluations of the photoreceptor layer on OCT images using software. Ooto and colleagues[26,28] described a method to define inner segment ellipsoid line disruption on SD-OCT (Spectralis) images as decreased reflectivity of the inner segment ellipsoid line in the fovea, and showed a significant association with the findings acquired by using adaptive optics scanning laser ophthalmoscopy in eyes with a healed macular hole. Wanek et al.[7] reported a method for automatic en face imaging of inner segment ellipsoid line by SD-OCT (Spectralis) and described findings in patients with various retinal diseases, including DME. Collectively, these studies demonstrate intensity-based inner segment ellipsoid line detection methods and show their clinical relevance. Although these methods are designed for good performance in the selective abstraction of inner segment ellipsoid line, they may not reflect information about photoreceptor-RPE complex alterations, other than discontinuity of the inner segment ellipsoid line, which we are focusing on.

Other groups showed the usefulness of PROS measurements. Forooghian et al.[19] used Cirrus HD-OCT (Carl Zeiss Meditec, Inc., Dublin, CA, USA) and reported a significant relationship between PROS thickness automatically measured using their prototype software and visual acuity in DME. Alasil et al.[18] used a Stratus OCT machine (Carl Zeiss Meditec, Inc.) and manually measured PROS thickness using custom software entitled "OCTOR," which allows for the precise positioning of prespecified boundaries on individual B-scans, and found a correlation with visual acuity. Although these studies show the clinical relevance of PROS measurements in DME, we speculate that PROS measurements also can reflect photoreceptor-RPE complex alterations other than discontinuity of the inner segment ellipsoid lines or ELM lines, such as hyperreflective foci in the outer retinal layers or bumpy RPE lines, as

Table 2. Association Between Photoreceptor Status and Parallelism of Photoreceptor-RPE Complex in OCT Images

	Parallelism	*P* Value	VA, logMAR	*P* Value
Inner segment ellipsoid line(+), $n = 13$	0.715 ± 0.078		0.073 ± 0.144	
Inner segment ellipsoid line(±), $n = 55$	0.598 ± 0.125		0.300 ± 0.234	
Inner segment ellipsoid line(−), $n = 22$	0.422 ± 0.119	<0.0001	0.680 ± 0.347	<0.0001
ELM line(+), $n = 35$	0.679 ± 0.100		0.176 ± 0.220	
ELM line(±), $n = 48$	0.520 ± 0.136		0.421 ± 0.298	
ELM line(−), $n = 7$	0.396 ± 0.102	<0.0001	0.862 ± 0.236	<0.0001
Hyperreflective foci in outer retinal layers				
Absent, $n = 49$	0.644 ± 0.131		0.206 ± 0.228	
Present, $n = 41$	0.486 ± 0.126	<0.0001	0.543 ± 0.325	<0.0001

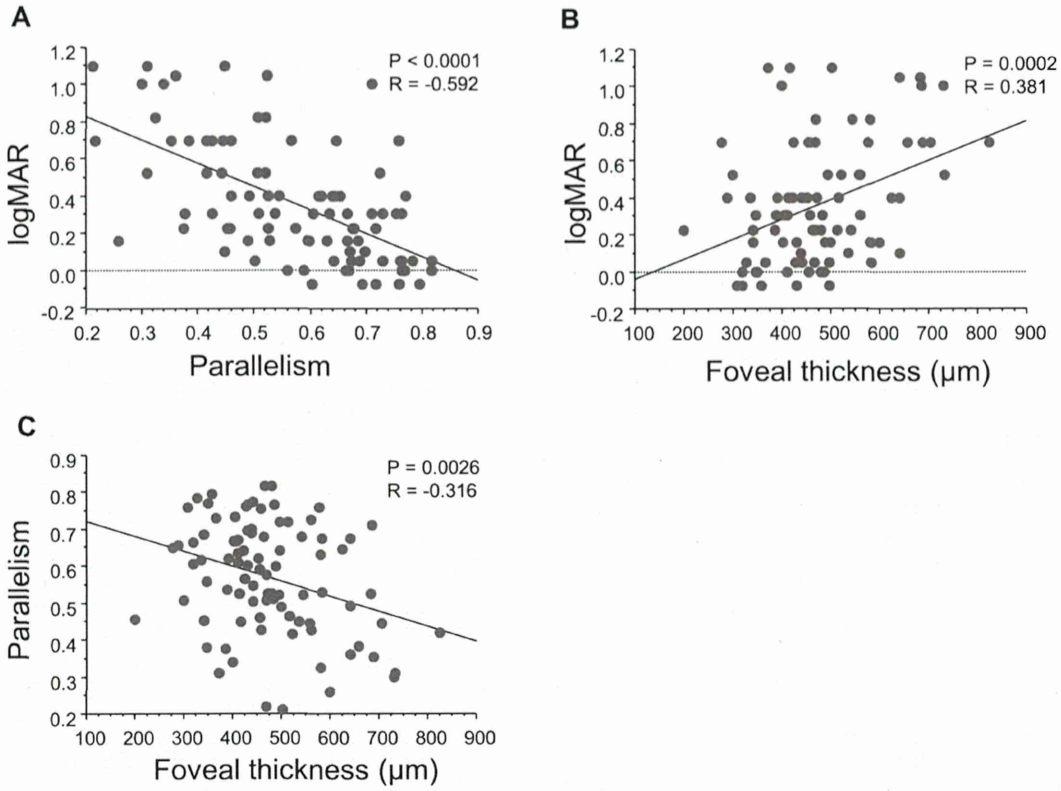

FIGURE 4. Correlations among VA, parallelism, and foveal thickness in patients with DME. (**A**) A significant negative correlation was shown between parallelism and logMAR VA ($R = -0.592$; $P < 0.0001$). (**B**) Foveal thickness demonstrated a modest correlation with logMAR VA ($R = 0.381$; $P = 0.0002$). (**C**) Significant negative correlations were found between parallelism and foveal thickness ($R = -0.316$; $P = 0.0316$).

is the case with parallelism, because PROS measurements have the potential to measure the deformation of lines as increased and decreased thicknesses. However, thickness measurements of small objects on OCT images require careful attention, in that the measurements may contain potential inaccuracies. Parallelism, which is based on a simple filtering process, is faithful to the original image and avoids problems associated with segmentation failure and picture interpolation to create solid segmentation lines.

Retinal thickness is a well-accepted parameter related to visual impairment in DME. In this study, parallelism showed a significant negative correlation with retinal thickness. This result supports the finding previously reported by Murakami et al.,[35] in which several relationships between the characteristics of the cystoid spaces and the photoreceptor changes beneath them were shown in DME for the first time. Parallelism, along with retinal thickness that can be calculated automatically with fewer segmentation errors, has the potential to shed light on the mechanism of photoreceptor changes in DME in future studies.

Our study has the following limitations: (1) We evaluated only horizontal and vertical scans for each subject without using the 3-dimensional scanning mode for full delineation. (2) This study was cross-sectional and retrospective in nature. Another longitudinal study should be planned in the future. (3) Parallelism is solely a marker for complexity. Considering that shape and size of the objects in the image depend on a degree of filtering, multiple objects can be extracted to produce a single fused object. Although the preprocessing methods were performed for all OCT images uniformly and the outcome of the current study was not considered to be biased, further improvement of the filtering process to bring computer recognition closer to human recognition is warranted.

In conclusion, parallelism is proposed as a new practical parameter for the complexity of photoreceptor-RPE complex alterations in DME. Parallelism was significantly lower in eyes with DME than in normal eyes, and correlated strongly with VA in eyes with DME. This parameter has the potential to reflect structural changes in photoreceptor layers, which include not only discontinuity of inner segment ellipsoid lines or ELM lines, but also other changes, such as the presence of hyperreflective foci.

Acknowledgments

Disclosure: **A. Uji**, None; **T. Murakami**, None; **N. Unoki**, None; **K. Ogino**, None; **T. Horii**, None; **S. Yoshitake**, None; **Y. Dodo**, None; **N. Yoshimura**, None

References

1. Saaddine JB, Honeycutt AA, Narayan KM, Zhang X, Klein R, Boyle JP. Projection of diabetic retinopathy and other major eye diseases among people with diabetes mellitus: United States, 2005-2050. *Arch Ophthalmol.* 2008;126:1740–1747.
2. Klein R, Klein BE, Moss SE, Cruickshanks KJ. The Wisconsin Epidemiologic Study of Diabetic Retinopathy. XV. The long-term incidence of macular edema. *Ophthalmology.* 1995;102:7–16.
3. Otani T, Kishi S. Tomographic findings of foveal hard exudates in diabetic macular edema. *Am J Ophthalmol.* 2001;131:50–54.

4. Hee MR, Puliafito CA, Wong C, et al. Quantitative assessment of macular edema with optical coherence tomography. *Arch Ophthalmol.* 1995;113:1019–1029.
5. Browning DJ, Glassman AR, Aiello LP, et al. Relationship between optical coherence tomography-measured central retinal thickness and visual acuity in diabetic macular edema. *Ophthalmology.* 2007;114:525–536.
6. Bandello F, Polito A, Del Borrello M, Zemella N, Isola M. "Light" versus "classic" laser treatment for clinically significant diabetic macular oedema. *Br J Ophthalmol.* 2005;89:864–870.
7. Martidis A, Duker JS, Greenberg PB, et al. Intravitreal triamcinolone for refractory diabetic macular edema. *Ophthalmology.* 2002;109:920–927.
8. Laursen ML, Moeller F, Sander B, Sjoelie AK. Subthreshold micropulse diode laser treatment in diabetic macular oedema. *Br J Ophthalmol.* 2004;88:1173–1179.
9. Ozdemir H, Karacorlu M, Karacorlu SA. Regression of serous macular detachment after intravitreal triamcinolone acetonide in patients with diabetic macular edema. *Am J Ophthalmol.* 2005;140:251–255.
10. Massin P, Duguid G, Erginay A, Haouchine B, Gaudric A. Optical coherence tomography for evaluating diabetic macular edema before and after vitrectomy. *Am J Ophthalmol.* 2003;135:169–177.
11. Kiernan DF, Mieler WF, Hariprasad SM. Spectral-domain optical coherence tomography: a comparison of modern high-resolution retinal imaging systems. *Am J Ophthalmol.* 2010;149:18–31.
12. Sakamoto A, Hangai M, Yoshimura N. Spectral-domain optical coherence tomography with multiple B-scan averaging for enhanced imaging of retinal diseases. *Ophthalmology.* 2008;115:1071–1078.e7.
13. Fleckenstein M, Charbel Issa P, Helb HM, et al. High-resolution spectral domain-OCT imaging in geographic atrophy associated with age-related macular degeneration. *Invest Ophthalmol Vis Sci.* 2008;49:4137–4144.
14. Murakami T, Nishijima K, Akagi T, et al. Segmentational analysis of retinal thickness after vitrectomy in diabetic macular edema. *Invest Ophthalmol Vis Sci.* 2012;53:6668–6674.
15. Marmor MF. Mechanisms of fluid accumulation in retinal edema. *Doc Ophthalmol.* 1999;97:239–249.
16. Spaide RF. Questioning optical coherence tomography. *Ophthalmology.* 2012;119:2203–2204.e1.
17. Sakamoto A, Nishijima K, Kita M, Oh H, Tsujikawa A, Yoshimura N. Association between foveal photoreceptor status and visual acuity after resolution of diabetic macular edema by pars plana vitrectomy. *Graefes Arch Clin Exp Ophthalmol.* 2009;247:1325–1330.
18. Alasil T, Keane PA, Updike JF, et al. Relationship between optical coherence tomography retinal parameters and visual acuity in diabetic macular edema. *Ophthalmology.* 2010;117:2379–2386.
19. Forooghian F, Stetson PF, Meyer SA, et al. Relationship between photoreceptor outer segment length and visual acuity in diabetic macular edema. *Retina.* 2010;30:63–70.
20. Maheshwary AS, Oster SF, Yuson RM, Cheng L, Mojana F, Freeman WR. The association between percent disruption of the photoreceptor inner segment-outer segment junction and visual acuity in diabetic macular edema. *Am J Ophthalmol.* 2010;150:63–67.e1.
21. Bolz M, Schmidt-Erfurth U, Deak G, Mylonas G, Kriechbaum K, Scholda C. Optical coherence tomographic hyperreflective foci: a morphologic sign of lipid extravasation in diabetic macular edema. *Ophthalmology.* 2009;116:914–920.
22. Uji A, Murakami T, Nishijima K, et al. Association between hyperreflective foci in the outer retina, status of photoreceptor layer, and visual acuity in diabetic macular edema. *Am J Ophthalmol.* 2012;153:710–717, 717.e1.
23. Nishijima K, Murakami T, Hirashima T, et al. Hyperreflective foci in outer retina predictive of photoreceptor damage and poor vision after vitrectomy for diabetic macular edema. *Retina.* 2014;34:732–740.
24. Ota M, Nishijima K, Sakamoto A, et al. Optical coherence tomographic evaluation of foveal hard exudates in patients with diabetic maculopathy accompanying macular detachment. *Ophthalmology.* 2010;117:1996–2002.
25. Murakami T, Nishijima K, Sakamoto A, Ota M, Horii T, Yoshimura N. Association of pathomorphology, photoreceptor status, and retinal thickness with visual acuity in diabetic retinopathy. *Am J Ophthalmol.* 2011;151:310–317.
26. Yokota S, Ooto S, Hangai M, et al. Objective assessment of foveal cone loss ratio in surgically closed macular holes using adaptive optics scanning laser ophthalmoscopy. *PLoS One.* 2013;8:e63786.
27. Wanek J, Zelkha R, Lim JI, Shahidi M. Feasibility of a method for en face imaging of photoreceptor cell integrity. *Am J Ophthalmol.* 2011;152:807–814. e1.
28. Ooto S, Hangai M, Takayama K, Ueda-Arakawa N, Hanebuchi M, Yoshimura N. Photoreceptor damage and foveal sensitivity in surgically closed macular holes: an adaptive optics scanning laser ophthalmoscopy study. *Am J Ophthalmol.* 2012;154:174–186.e2.
29. Murakami T, Yoshimura N. Structural changes in individual retinal layers in diabetic macular edema. *J Diabetes Res.* 2013;2013:920713.
30. Uji A, Murakami T, Unoki N, et al. Parallelism as a novel marker for structural integrity of retinal layers in optical coherence tomographic images in eyes with epiretinal membrane. *Am J Ophthalmol.* 2014;157:227–236.e4.
31. Murakami T, Nishijima K, Sakamoto A, Ota M, Horii T, Yoshimura N. Foveal cystoid spaces are associated with enlarged foveal avascular zone and microaneurysms in diabetic macular edema. *Ophthalmology.* 2011;118:359–367.
32. Yoneda A, Higaki T, Kutsuna N, et al. Chemical genetic screening identifies a novel inhibitor of parallel alignment of cortical microtubules and cellulose microfibrils. *Plant Cell Physiol.* 2007;48:1393–1403.
33. Ueda H, Yokota E, Kutsuna N, et al. Myosin-dependent endoplasmic reticulum motility and F-actin organization in plant cells. *Proc Natl Acad Sci U S A.* 2010;107:6894–6899.
34. Otsu N. A threshold selection method form gray-level histograms. *IEEE Trans Syst Man Cybern.* 1979;9:62–66.
35. Murakami T, Nishijima K, Akagi T, et al. Optical coherence tomographic reflectivity of photoreceptors beneath cystoid spaces in diabetic macular edema. *Invest Ophthalmol Vis Sci.* 2012;53:1506–1511.

Investigative Ophthalmology & Visual Science

Parallelism as a Novel Marker for Structural Integrity of Retinal Layers in Optical Coherence Tomographic Images in Eyes With Epiretinal Membrane

AKIHITO UJI, TOMOAKI MURAKAMI, NORIYUKI UNOKI, KEN OGINO, KAZUAKI NISHIJIMA, SHIN YOSHITAKE, YOKO DODO, AND NAGAHISA YOSHIMURA

• PURPOSE: To propose a new parameter, "Parallelism," to evaluate retinal layer integrity on spectral-domain optical coherence tomography (SDOCT), and to investigate the association between parallelism and visual function in eyes with idiopathic epiretinal membrane (ERM).
• DESIGN: Retrospective, observational evaluation of a diagnostic test.
• METHODS: We evaluated a consecutive series of 57 eyes of 57 patients with ERM and 30 healthy eyes of 30 volunteers for whom M-CHARTS testing and SDOCT were performed on the same day. OCT images were skeletonized, and the orientation of segmented lines in the image was termed "Parallelism" and was expressed as a value ranging from 0-1 and increasing as the retinal layers ran more parallel with each other. The relationships between parallelism and visual acuity and between parallelism and metamorphopsia score were evaluated.
• RESULTS: In normal eyes, parallelism was nearly homogeneous and varied slightly with the location. Parallelism in eyes with ERM was significantly lower than that in normal eyes. In the horizontal and vertical scans, parallelism was significantly correlated with visual acuity, horizontal metamorphopsia score, and vertical metamorphopsia score. Parallelism of the center (1 mm) in the horizontal scan was strongly correlated with horizontal metamorphopsia score ($R = -0.632$; $P < .0001$). Significant negative correlation was found between parallelism and retinal thickness both in horizontal and vertical scans.
• CONCLUSIONS: Parallelism was significantly lower in eyes with ERM than in normal eyes, and correlated strongly with metamorphopsia and visual acuity in eyes with ERM. (Am J Ophthalmol 2014;157:227–236.

AJO.com Supplemental Material available at AJO.com.
Accepted for publication Sep 3, 2013.
From the Department of Ophthalmology and Visual Sciences, Kyoto University Graduate School of Medicine, Kyoto, Japan.
Inquiries to Akihito Uji, Department of Ophthalmology and Visual Sciences, Kyoto University Graduate School of Medicine, 54 Shogoin Kawahara-cho, Sakyo-ku, Kyoto 606-8507, Japan; e-mail: akihito1@kuhp.kyoto-u.ac.jp

IN RECENT DECADES, IMAGING TECHNOLOGY IN OPTICAL coherence tomography (OCT) has advanced rapidly and contributed immeasurably to progress in ophthalmology.[1] OCT provides cross-sectional images of the retina, as in microscopy of tissue sections, and a 3-dimensional standpoint in understanding retinal diseases.[2–4] OCT also enables objective measurement of retinal thickness as a novel quantitative parameter for assessment of disease severity and evaluation of therapeutic efficacy.[5,6]

More recently, improved OCT image quality has been achieved by increased retinal scan speed owing to advancement of OCT generations from time-domain OCT to spectral-domain OCT (SDOCT) and by image processing techniques using multiple-aligned OCT scans to reduce speckle noise.[7–10] Later generations of OCT systems have enabled clinicians to appreciate the individual retinal layers, and these layers on the OCT images have provided important information about pathologies of diseases such as diabetic macular edema,[11] epiretinal membrane (ERM),[12–14] and glaucoma.[15–17] Quantitative evaluation of disrupted retinal layers by layer segmentation, which allows analysis of continuous sequence in retinal thickness between selected layers, has yielded correlations between local layer thickness and pathologic conditions.[18–22] However, use of software-based automatic layer segmentation analysis in clinical practice is limited to specific diseases because of inaccuracy in certain cases.[19,23] Automatic layer segmentation software functions effectively in normal OCT images and uncomplicated OCT images in diseased eyes, such as in glaucoma and retinitis pigmentosa, but manual compensation is sometimes required for analyses of segmented lines in OCT images in diseased eyes.[24] Developments of robust software for segmentation analyses are eagerly expected.

In this study, we proposed a new parameter, "Parallelism," to evaluate retinal layer integrity by using an entirely new concept.[25,26] Parallelism indicates how straight the layers are and how parallel the layers are to each other. It can be calculated using line segments obtained by simply filtering and thresholding of the original image, while segmentation analysis requires solid lines to calculate retinal thickness. Picture interpolation to create solid lines is unnecessary; therefore, parallelism has potential as a robust and easily determined parameter of structural integrity of retinal layers. The algorithm for

0002-9394/$36.00
http://dx.doi.org/10.1016/j.ajo.2013.09.008

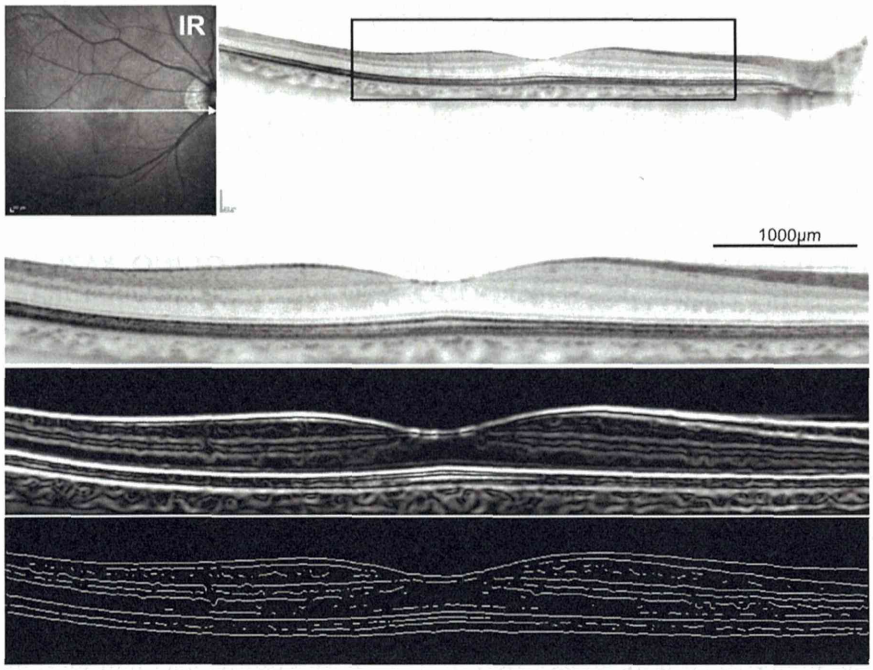

FIGURE 1. Extraction of skeletonized image from retinal layers in optical coherence tomographic images. Images of the right eye of a 52-year-old woman from our database of normal volunteers. (Top row) Horizontal line through the fovea in the infrared (IR) spectral-domain optical coherence tomography (SDOCT) image. (Second row) SDOCT image of section 6 mm in length outlined in black in top row. (Third row) Filtered image of second row after application of derivative of a Gaussian filter for edge detection. (Bottom row) Skeletonized SDOCT image generated from third row through band-pass filtration and binarization by intensity thresholding. Lines in the vitreous space and outside the retinal pigment epithelium have been erased manually as artifacts. Each line segment represents orientation of the striped pattern in the retina. Parallelism calculated for the 6-mm section, full thickness of the center (1 mm), inner layer of the center (1 mm), and outer layer of the center (1 mm) was 0.914, 0.925, 0.868, and 0.954, respectively.

calculating parallelism was tested using OCT scans from normal subjects and patients with ERM, and clinical relevance was explored.

METHODS

• **SUBJECTS:** The present study had a retrospective, observational design for evaluation of a diagnostic test. All the research and measurements adhered to the tenets of the Declaration of Helsinki and were approved by the Institutional Review Board of Kyoto University Graduate School of Medicine for retrospective review of existing patient data. We retrospectively examined 57 eyes of 57 patients (mean age ± standard deviation, 67.5 ± 7.6 years; range, 50-81 years) with idiopathic ERM but without any other macular abnormality who visited Kyoto University Hospital from February 19, 2013 through July 31, 2013. The inclusion criterion was the availability of M-CHARTS (Inami Co, Tokyo, Japan) test results and SDOCT images of sufficient quality that were acquired on the same day. Eyes with secondary ERM (eg, attributable to diabetic retinopathy, venous occlusion, retinal detachment, uveitis, or trauma) were excluded from this study. All patients had undergone comprehensive ophthalmologic examinations, including measurement of best-corrected visual acuity (BCVA), slit-lamp biomicroscopy, color fundus photography, and SDOCT. Patients were tested at this same visit for the presence of metamorphopsia by using M-CHARTS to obtain separate measurements of the severity of image distortion along horizontal and vertical lines. Data of 30 eyes of 30 volunteers (64.5 ± 10.7 years; range, 38-77 years) for candidate control eyes were retrospectively collected from our database of normal volunteers.

• **OPTICAL COHERENCE TOMOGRAPHY:** Retinal sectional images of the macula were obtained using SDOCT (Spectralis; Heidelberg Engineering, Heidelberg, Germany). The central fovea was defined as the area lacking inner retinal layers in the macular region.[27] Cross-sectional images at 30 degrees through the fovea were chosen for each eye. The Spectralis OCT system has built-in software to calculate retinal thickness, and we used this feature to measure average foveal thickness of the area 6 mm in diameter centered on the fovea and of each subfield. Scans were manually corrected if there were any B-scans with an algorithm failure, such as inaccurately drawn automated boundary lines.

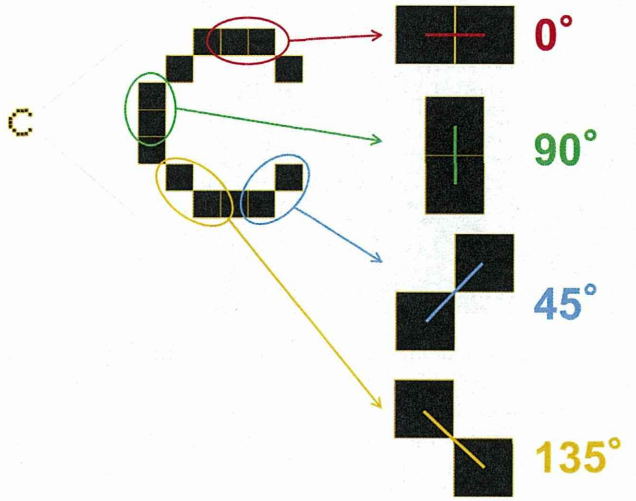

FIGURE 2. Example of calculation of parallelism. A digital representation of the letter "C," which consists of 13 pixels, is used for calculation of parallelism. In digital images, pixels are adjoined to each other in 45-degree increments in 8 different directions and angles of a neighboring pixel pair can be categorized as 0 (red), 45 (blue), 90 (green), and 135 degrees (yellow) against the horizon. In this study, parallelism is calculated as follows: Parallelism = $(|n_0 - n_{90}| + |n_{45} - n_{135}|)/(n_0 + n_{45} + n_{90} + n_{135})$, where n_0, n_{45}, n_{90}, and n_{135} are the numbers of pixel pairs at 0, 45, 90, and 135 degrees, respectively. Parallelism can range from 0-1 and increases as the retinal layers run more parallel with each other. In analysis of a curved segment, parallelism is equivalent to the ratio of straight-line distance between the starting point and end point to the whole length of the curved segments. However, in this study, parallelism is designed to count discretization of the angle in 45-degree increments in the case of multiple line segments in the image, which is not in strict accordance with the above-mentioned definition. In the example, $n_0 = 4$, $n_{45} = 3$, $n_{90} = 2$, and $n_{135} = 3$, and parallelism = 0.167.

• CALCULATION OF PARALLELISM: To quantitatively evaluate orientations of retinal layers, we first extracted skeletonized images (line art) from OCT images by applying filtration through first-order derivative of a Gaussian filter using the ImageJ plug-in Feature Detector, an algorithm based on the optimization of a Canny-like criterion,[28–31] followed by a 1-2 pixel band-pass filter and binarization by intensity thresholding using Otsu's thresholding method for automatic binarization level decision (Figure 1).[25,26,32] Because the target object of image processing in this study was a 6-mm-long section on a full-thickness OCT image, filter bandwidth was adjusted to reduce noise in the images with maintenance of visualization of multiple layers. Lines in the vitreous space and beyond the retinal pigment epithelium were erased manually as artifacts. ERMs were not erased and were included in analyses. Note that the analysis requires only information regarding layer orientation, which can be obtained using line segments, and not solid lines or accurate segmentation of the retinal layers.

In the skeletonized images, angles of neighboring pixel pairs against the horizon were categorized as 0, 45, 90, and 135 degrees, and the numbers of pixel pairs were counted, basically according to the study by Ueda and associates on actin filament-bundle orientations in plants (Figure 2).[26] In this study, "Parallelism" referred to the orientations of retinal layers and was calculated using the ImageJ plug-in KbiLinesAngle (http://hasezawa.ib.k.u-tokyo.ac.jp/zp/Kbi/ImageJKbiPlugins), as follows:

$$\text{Parallelism} = (|n_0 - n_{90}| + |n_{45} - n_{135}|)/(n_0 + n_{45} + n_{90} + n_{135})$$

where n_0, n_{45}, n_{90}, and n_{135} are the numbers of pixel pairs orientated at 0, 45, 90, and 135 degrees, respectively.[25,26] Parallelism ranges from 0-1 and increases as the retinal layers run more parallel with each other. All digital images were processed by a single operator (A.U.) using ImageJ (developed by Wayne Rasband, National Institutes of Health, Bethesda, Maryland, USA; available at http://rsb.info.nih.gov/ij/index.html) and its plug-in software.

Parallelism was calculated in an area 6 mm in length centered on the fovea and in the following 5 subfields: center (1 mm), 2 parafovea (0.5-1.5 mm), and 2 perifovea (1.5-3.0 mm) (Figure 3). Furthermore, in each subfield, parallelism was calculated in the area above the outer nuclear layer (ONL) space as the inner layer and in the area below the ONL space as the outer layer.[33]

• STATISTICAL ANALYSIS: All values are expressed as the mean ± standard deviation. All BCVA measurements were converted to logarithm of the minimal angle of resolution (logMAR) equivalents before statistical analysis. Student *t* tests were used to compare the 2 groups (normal subjects vs ERM patients) regarding age, logMAR VA, parallelism, and retinal thickness. Comparisons of parallelism and retinal thickness of the 5 subfields were carried out using repeated-measures analysis of variance, and differences between the 2 groups were analyzed using the paired *t* test followed by Bonferroni correction. Associations of metamorphopsia scores with parallelism and retinal thickness and of logMAR VA with parallelism and retinal thickness were analyzed using the Pearson correlation coefficient. Stepwise regression analysis was performed to evaluate the contribution made by parallelism and retinal thickness of the 5 subfields to the horizontal metamorphopsia score, vertical metamorphopsia score, and logMAR VA. Furthermore, correlation between parallelism and retinal thickness was analyzed using the Pearson correlation coefficient. A *P* value of $<.05$ was considered statistically significant. All analyses, except for multiple linear regression analysis, were performed using StatView (version 5.0; SAS Institute, Cary, North Carolina, USA). Stepwise regression analysis was performed using SPSS (Version 17; GraphPad Software, La Jolla, California, USA).

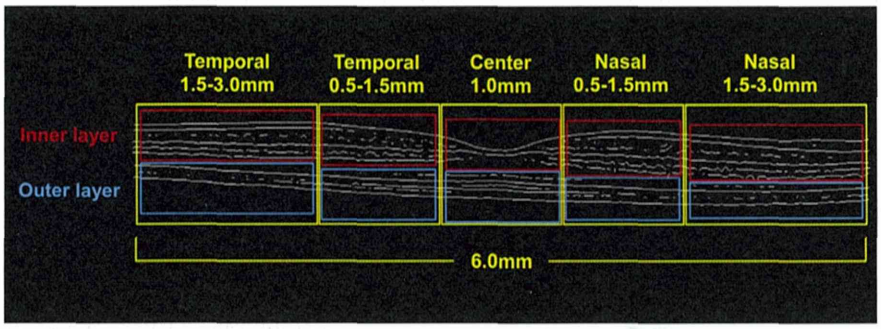

FIGURE 3. Regions of interest in skeletonized retinal layers in horizontal line scan of optical coherence tomographic image. Parallelism was calculated in a 6-mm-long area centered on the fovea and also in the 5 subfields: center (1 mm), 2 parafovea (temporal and nasal, 0.5-1.5 mm), and 2 perifovea (temporal and nasal, 1.5-3.0 mm). Furthermore, in each subfield, parallelism was calculated in the area above the outer nuclear layer (ONL) space as the inner layer and the area below the ONL space as the outer layer. Regions of interest in the skeletonized vertical line scan were similarly set on the image as follows: center (1 mm), 2 parafovea (inferior and superior, 0.5-1.5 mm), and 2 perifovea (inferior and superior, 1.5-3.0 mm).

RESULTS

SIX HORIZONTAL AND 7 VERTICAL SCANS OUT OF 57 SCAN pairs of ERM patients were excluded from the analyses because the central fovea could not be identified. A pair of horizontal and vertical scans in an ERM patient was also excluded from the analyses because of low image quality. Finally, skeletonized images were successfully obtained from the remaining 50 horizontal scans and 49 vertical scans of ERM patients and the 30 scan pairs of volunteers through semi-automatic image processing (Figures 1 and 4).

• PARALLELISM IN NORMAL SUBJECTS: Parallelism of normal subjects is shown in Table 1. In the horizontal scan, there were significant differences in full-thickness parallelism ($P = .0090$) and in inner-layer parallelism ($P < .0001$) among 5 subfields; however, significant differences were not shown in outer-layer parallelism among 5 subfields ($P = .0966$) (Supplemental Figure 1, available at AJO.com). In the vertical scan, significant differences were disclosed in full-thickness, inner-layer, and outer-layer parallelism values. Compared with the horizontal scan, parallelism of the perifovea (1.5-3.0 mm) tended to be lower than that of other subfields, and significant differences in full-thickness and outer-layer parallelism values were observed between the perifovea and some of the other subfields (Supplemental Figure 2, available at AJO.com). Vessel shadows were imaged as lines perpendicular to the retinal layers in skeletonized vertical scans, which might have decreased parallelism in the perifovea (Supplemental Figure 3, available at AJO.com). Retinal thickness was smallest in the center (1 mm) and greatest in the parafovea (0.5-1.5 mm) both in horizontal and in vertical scans.

• DIFFERENCES IN PARALLELISM BETWEEN NORMAL SUBJECTS AND PATIENTS WITH EPIRETINAL MEMBRANE: In many cases of ERM, line segments around the fovea were depicted in random directions, which probably contributed to decreased parallelism (Figure 4). Significant differences were observed in full-thickness parallelism between normal eyes and eyes with ERM except for the perifovea (inferior, 1.5-3.0 mm) in the vertical scan (Table 1). In the inner layer, parallelism was significantly lower in eyes with ERM than in normal eyes. In the outer layer, no significant differences were noted between the groups except for parallelism of the center (1 mm) in both the horizontal and vertical scans and parallelism of the perifovea (superior, 1.5-3.0 mm) in the vertical scan. Retinal thicknesses were significantly higher in eyes with ERM than in normal eyes.

• CORRELATION BETWEEN VISUAL FUNCTION AND PARALLELISM IN PATIENTS WITH EPIRETINAL MEMBRANE: In the horizontal scan, parallelism in the areas excluding the perifovea (nasal, 1.5-3.0 mm) correlated significantly with visual acuity and horizontal metamorphopsia score (Table 2). In particular, parallelism of the center (1 mm) had a strong correlation with horizontal metamorphopsia score ($R = -0.632$; $P < .0001$). Significant correlations were also found in all 5 subfields between parallelism and vertical metamorphopsia score. In the individual analysis of inner and outer layers, parallelism significantly correlated with horizontal and vertical metamorphopsia scores.

In the vertical scan, parallelism in the areas excluding the perifovea (inferior, 1.5-3.0 mm) was also significantly correlated with visual acuity and horizontal metamorphopsia score. Furthermore, parallelism had a correlation with vertical metamorphopsia score. Inner-layer parallelism correlated significantly with visual acuity, horizontal metamorphopsia score, and vertical metamorphopsia score in some of the subfields including the center (1 mm), while outer-layer parallelism showed a significant correlation between some of the subfields excluding the center (1 mm) and metamorphopsia score or visual acuity.

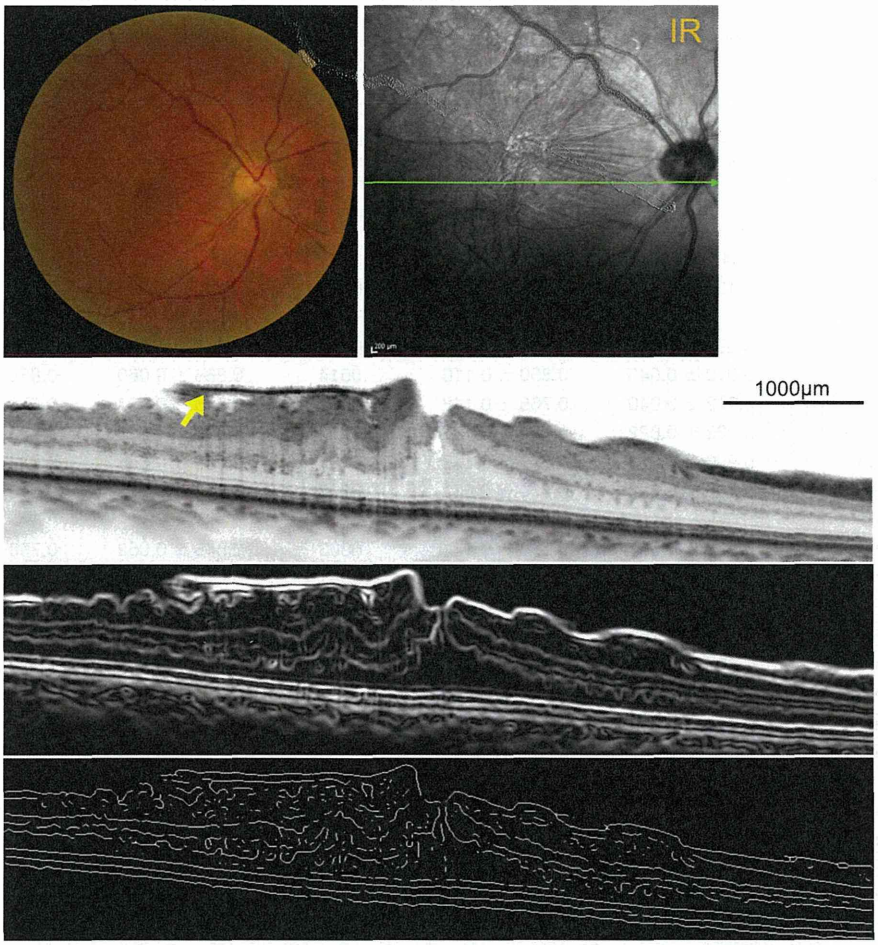

FIGURE 4. Extraction of skeletonized image from retinal layers in optical coherence tomographic images of patient with epiretinal membrane (ERM). Images of the right eye of a 55-year-old man with an idiopathic ERM. Snellen equivalent best-corrected visual acuity was 20/20 in this eye, and M-CHARTS metamorphopsia scores were 0.8 for horizontal lines and 1.1 for vertical lines. (Top left) Color fundus photograph shows retinal folds and irregular reflex in the fovea. (Top right) Infrared (IR) image clearly shows retinal folds, irregular reflex, and distortion of retinal vessels. (Second row) Spectral-domain optical coherence tomography (SDOCT) image of 6-mm-long section cropped from the horizontal line scan of the SDOCT image through the fovea in the direction of the horizontal arrow in top right panel shows the ERM (arrow) and distortions of retinal layers. (Third row) Filtered image of second row after application of derivative of a Gaussian filter for edge detection. (Bottom row) Skeletonized SDOCT image generated from third row. Segmented lines that are aligned randomly represent distorted layers in the original OCT image and are used to calculate parallelism. Parallelism calculated for the 6-mm section, full thickness of the center (1 mm), inner layer of the center (1 mm), and outer layer of the center (1 mm) was 0.833, 0.655, 0.344, and 0.947, respectively.

• CORRELATION BETWEEN VISUAL FUNCTION AND RETINAL THICKNESS IN PATIENTS WITH EPIRETINAL MEMBRANE: Retinal thickness correlated significantly with visual acuity and vertical and horizontal metamorphopsia scores in some of the subfields, including the center (1 mm) in both horizontal and vertical scans (Table 2).

• CORRELATION BETWEEN PARALLELISM AND RETINAL THICKNESS IN PATIENTS WITH EPIRETINAL MEMBRANE: Significant negative correlations were found between full-thickness and inner-layer parallelism and retinal thickness in all subfields of horizontal and vertical scans (Table 3). Multiple significant correlations were also found between outer-layer parallelism and retinal thickness in some of the subfields of horizontal and vertical scans.

• MULTIVARIATE ANALYSIS: Analysis included 10 independent variables (full-thickness parallelism in 5 subfields and retinal thickness in 5 subfields).

In the horizontal scan, significant associations were found between parallelism of the center (1 mm) and horizontal metamorphopsia score ($\beta = -0.632$, $P < .001$), vertical metamorphopsia score ($\beta = -0.487$, $P < .001$), and visual acuity ($\beta = -0.522$, $P < .001$).

In the vertical scan, parallelism of the parafovea (inferior, 0.5-1.5 mm) correlated with horizontal

TABLE 1. Differences in Parallelism of Retinal Layers in Optical Coherence Tomographic Images Between Normal Subjects and Patients With Epiretinal Membrane

Characteristic	Horizontal Scan			Vertical Scan		
	Normal Eyes	Eyes With ERM	*P* Value	Normal Eyes	Eyes With ERM	*P* Value
No. eyes/patients	30/30	50/50	-	30/30	49/49	-
Men/women	18/12	24/26	-	18/12	24/25	-
Age (y)	64.5 ± 10.7	67.8 ± 7.5	.1141	64.5 ± 10.7	68.4 ± 7.2	.0549
Visual acuity (logMAR)	−0.150 ± 0.044	0.172 ± 0.206	<.0001	−0.150 ± 0.044	0.174 ± 0.205	<.0001
Parallelism full thickness						
6 mm	0.896 ± 0.034	0.800 ± 0.101	<.0001	0.857 ± 0.035	0.766 ± 0.093	<.0001
T or I, 1.5-3.0 mm	0.919 ± 0.043	0.850 ± 0.110	.0014	0.866 ± 0.060	0.839 ± 0.092	.1570
T or I, 0.5-1.5 mm	0.902 ± 0.040	0.765 ± 0.148	<.0001	0.875 ± 0.054	0.759 ± 0.119	<.0001
Center, 1.0 mm	0.922 ± 0.022	0.761 ± 0.135	<.0001	0.900 ± 0.029	0.735 ± 0.141	<.0001
N or S, 0.5-1.5 mm	0.903 ± 0.036	0.791 ± 0.117	<.0001	0.883 ± 0.054	0.736 ± 0.138	<.0001
N or S, 1.5-3.0 mm	0.908 ± 0.036	0.879 ± 0.062	.0208	0.862 ± 0.061	0.816 ± 0.116	.0466
Parallelism inner layer						
T or I, 1.5-3.0 mm	0.891 ± 0.057	0.789 ± 0.141	.0003	0.848 ± 0.052	0.798 ± 0.097	.0105
T or I, 0.5-1.5 mm	0.856 ± 0.063	0.667 ± 0.195	<.0001	0.840 ± 0.050	0.687 ± 0.144	<.0001
Center, 1.0 mm	0.839 ± 0.048	0.619 ± 0.185	<.0001	0.804 ± 0.056	0.592 ± 0.194	<.0001
N or S, 0.5-1.5 mm	0.867 ± 0.052	0.714 ± 0.154	<.0001	0.850 ± 0.057	0.658 ± 0.167	<.0001
N or S, 1.5-3.0 mm	0.897 ± 0.037	0.854 ± 0.071	.0029	0.852 ± 0.053	0.778 ± 0.130	.0038
Parallelism outer layer						
T or I, 1.5-3.0 mm	0.958 ± 0.044	0.963 ± 0.037	.5906	0.903 ± 0.072	0.930 ± 0.075	.1269
T or I, 0.5-1.5 mm	0.964 ± 0.023	0.953 ± 0.037	.1692	0.940 ± 0.046	0.932 ± 0.051	.4590
Center, 1.0 mm	0.965 ± 0.017	0.939 ± 0.043	.0024	0.956 ± 0.022	0.942 ± 0.030	.0343
N or S, 0.5-1.5 mm	0.959 ± 0.025	0.946 ± 0.032	.0541	0.949 ± 0.034	0.927 ± 0.059	.0788
N or S, 1.5-3.0 mm	0.947 ± 0.038	0.957 ± 0.031	.2093	0.887 ± 0.082	0.939 ± 0.047	.0006
Retinal thickness						
T or I, 1.5-3.0 mm	281 ± 14	338 ± 49	<.0001	283 ± 11	310 ± 42	<.0001
T or I, 0.5-1.5 mm	320 ± 13	430 ± 59	<.0001	338 ± 11	418 ± 55	<.0001
Center, 1.0 mm	251 ± 16	457 ± 82	<.0001	257 ± 19	454 ± 80	<.0001
N or S, 0.5-1.5 mm	337 ± 12	435 ± 60	<.0001	343 ± 12	427 ± 68	<.0001
N or S, 1.5-3.0 mm	315 ± 13	353 ± 49	<.0001	301 ± 13	344 ± 47	.0001

ERM = epiretinal membrane; I = inferior; LogMAR = logarithm of minimal angle of resolution; N = nasal; S = superior; T = temporal.

metamorphopsia score (ß = −0.465, $P = .001$) and vertical metamorphopsia score (ß = −0.524, $P < .001$). Visual acuity correlated with retinal thickness of the center (1 mm) (ß = 0.486, $P = .001$).

DISCUSSION

THE AIM OF THIS STUDY WAS TO FIND A NEW ROBUST AND practical surrogate marker, other than retinal thickness, for evaluation of retinal layer integrity. Study results demonstrated that "Parallelism," a parameter reflecting layer orientation, could be obtained using line segments in skeletonized OCT images and was clinically relevant in eyes with ERM. To the best of our knowledge, this is the first study that employed layer orientation in OCT image analysis.

In normal eyes, full-thickness parallelism, unlike retinal thickness, was nearly homogeneous, with slight variations according to location. Meanwhile, inner-layer parallelism had the smallest value in the center (1 mm) and outer-layer parallelism underwent very little change except at the perifovea (1.5-3.0 mm), where values were extremely small in the vertical scan, which might have been caused by vessel shadows imaged as lines perpendicular to the retinal layers. These results are thought to be attributable to the existence of the fovea at which the inner layers converge. Because vertical OCT scans include relatively large vessels in the areas of the perifovea (1.5-3.0 mm), which are not visualized in horizontal OCT scans, we suggest excluding these areas in the analysis of parallelism to remove artifacts.

Significant differences between normal eyes and eyes with ERM, and significant correlations with visual function, were detected in both parallelism and retinal thickness. Moreover, parallelism was strongly correlated with retinal thickness in ERM patients, suggesting that parallelism was comparative to retinal thickness in evaluation